

# Nonzero $\theta_{13}$ and $CP$ violation in a model with $A_4$ flavor symmetry

Y. H. Ahn\*

*School of Physics, KIAS, Seoul 130-722, Korea*

Sin Kyu Kang†

*Institute of Convergence Fundamental Studies and School of Liberal Arts, Seoul-Tech, Seoul 139-743, Korea*  
 (Received 24 April 2012; published 2 November 2012)

Motivated by recent observations of nonzero  $\theta_{13}$  from the Daya Bay and RENO experiments, we propose a renormalizable neutrino model with  $A_4$  discrete symmetry accounting for deviations from the tri-bimaximal mixing pattern of the neutrino mixing matrix indicated by neutrino oscillation data. In the model, the light neutrino masses can be generated by radiative corrections, and we show how the light neutrino mass matrix can be diagonalized by the Pontecorvo-Maki-Nakagawa-Sakata mixing matrix whose entries are determined by the current neutrino data, including the Daya Bay result. We show that the origin of the deviations from the tri-bimaximal mixing is nondegeneracy of the neutrino Yukawa coupling constants, and unremovable  $CP$  phases in the neutrino Yukawa matrix give rise to both low energy  $CP$  violation measurable from neutrino oscillation and high energy  $CP$  violation.

 DOI: [10.1103/PhysRevD.86.093003](https://doi.org/10.1103/PhysRevD.86.093003)

PACS numbers: 14.60.Pq, 12.60.Fr, 14.60.St

## I. INTRODUCTION

Very recently, the Daya Bay Collaboration [1] announced  $5.2\sigma$  observation of the nonzero mixing angle  $\theta_{13}$  with the result given by  $\sin^2 2\theta_{13} = 0.092 \pm 0.016(\text{stat}) \pm 0.005(\text{syst})$ .<sup>1</sup> This result is in good agreement with the previous data from the T2K, MINOS, and Double Chooz Collaborations [3], and the progress from Daya Bay and RENO have led us to accomplish the measurements of three mixing angles,  $\theta_{12}$ ,  $\theta_{23}$ , and  $\theta_{13}$ , from three kinds of neutrino oscillation experiments. A combined analysis of the data coming from T2K, MINOS, Double Chooz, and Daya Bay experiments shows [4] that

$$\sin^2 2\theta_{13} = 0.089 \pm 0.016(0.047), \quad (1)$$

or equivalently

$$\theta_{13} = 8.68_{-0.84}^{+0.77}({}_{-2.76}^{+2.14})^\circ \quad (2)$$

at  $1\sigma$  ( $3\sigma$ ) levels and that the hypothesis  $\theta_{13} = 0$  is now rejected at a significance level higher than  $6\sigma$ . In addition to the measurement of the mixing angle  $\theta_{13}$ , the global fit of the neutrino mixing angles and mass-squared differences at  $1\sigma$  ( $3\sigma$ ) levels are given by [5]

$$\begin{aligned} \theta_{12} &= 34.0_{-0.9}^{+1.0}({}_{-2.7}^{+2.9})^\circ, \\ \theta_{23} &= 46.1_{-4.0}^{+3.5}({}_{-7.5}^{+7.0})^\circ, \\ \theta_{13} &= \begin{cases} 6.5_{-1.4}^{+1.6}({}_{-4.7}^{+4.2})^\circ, & \text{NH} \\ 7.3_{-1.5}^{+1.7}({}_{-5.5}^{+4.1})^\circ, & \text{IH} \end{cases} \quad (3) \\ \Delta m_{21}^2 [10^{-5} \text{ eV}^2] &= 7.59_{-0.18}^{+0.20}({}_{-0.50}^{+0.60}), \\ \Delta m_{31}^2 [10^{-3} \text{ eV}^2] &= \begin{cases} 2.50_{-0.16}^{+0.09}({}_{-0.36}^{+0.26}), & \text{NH} \\ 2.40_{-0.09}^{+0.08}({}_{-0.27}^{+0.27}), & \text{IH} \end{cases} \end{aligned}$$

in which NH and IH stand for the normal hierarchical neutrino spectrum and the inverted one, respectively. The data in Eqs. (2) and (3) strongly support that the tri-bimaximal (TBM) mixing pattern of the lepton mixing matrix [6] should be modified. There have been theoretical attempts to explain what causes the three mixing angles to deviate from their TBM values [7].

Motivated by the measurements of  $\theta_{13}$  from the Daya Bay and RENO experiments, we propose in this paper a renormalizable model with  $A_4$  discrete symmetry which gives rise to deviations from the TBM mixing indicated by the current neutrino data. In addition to the leptons and the Higgs scalar of the standard model (SM), the model we propose contains three right-handed heavy Majorana neutrinos and several scalar fields which are electroweak singlets required to construct desirable forms of the leptonic mass matrices. Although we introduce electroweak singlet heavy Majorana neutrinos, the usual seesaw mechanism does not operate because the scalar field involved in neutrino Yukawa terms cannot get vacuum expectation value (VEV). However, as will be shown later, the light neutrino masses can be generated through loop corrections, which are a kind of so-called radiative seesaw mechanism

\*yhahn@kias.re.kr

†skkang@snut.ac.kr

<sup>1</sup>The RENO Collaboration also announced observation of the nonzero mixing angle  $\theta_{13}$  [2] in agreement with the result from the Daya Bay Collaboration.

[8]. In the paper, we will show how the light neutrino mass matrix generated through loop corrections can be diagonalized by the Pontecorvo-Maki-Nakagawa-Sakata (PMNS) mixing matrix whose entries are determined by the current neutrino data. The origin of the deviations from TBM mixing in our model is nondegeneracy of the neutrino Yukawa coupling constants among three generations, which is different from other attempts to explain the deviations from the TBM mixing [7].

Since a nontrivial Dirac  $CP$  phase can exist only when the mixing angle  $\theta_{13}$  has nonzero value in the standard parametrization of the leptonic mixing matrix, the observations of nonzero  $\theta_{13}$  from the Daya Bay and RENO experiments shed light on the search for  $CP$  violation in the leptonic sector. We will show that unremovable  $CP$  phases in the neutrino Yukawa matrix are the origin of the low energy  $CP$  violation measurable from neutrino oscillation as well as high energy  $CP$  violation. Therefore, we can anticipate that there may exist some correlation between low energy  $CP$  violation and high energy  $CP$  violation.

## II. MODEL WITH $A_4$ SYMMETRY

The model we consider is the standard model (SM), extended to contain three right-handed  $SU(2)_L$ -singlet Majorana neutrinos,  $N_R$ . In addition to the usual SM Higgs doublet  $\Phi$ , we newly introduce two scalar fields,  $\chi$  and  $\eta$ , that are singlet and doublet under  $SU(2)_L$ , respectively:

$$\Phi = (\varphi^+, \varphi^0)^T, \quad \chi, \quad \eta = (\eta^+, \eta^0)^T. \quad (4)$$

In order to account for the present neutrino oscillation data, we impose  $A_4$  flavor symmetry for leptons and scalars. In addition to  $A_4$  symmetry, we introduce extra auxiliary  $Z_2$  symmetry so that a radiative seesaw at around TeV scale should operate. Here we recall that  $A_4$  is the symmetry group of the tetrahedron and the finite groups of the even permutation of four objects [9]. The group  $A_4$  has two generators  $S$  and  $T$ , satisfying the relation  $S^2 = T^3 = (ST)^3 = \mathbf{1}$ . In the three-dimensional unitary representation,  $S$  and  $T$  are given by

$$S = \begin{pmatrix} 1 & 0 & 0 \\ 0 & -1 & 0 \\ 0 & 0 & -1 \end{pmatrix}, \quad T = \begin{pmatrix} 0 & 1 & 0 \\ 0 & 0 & 1 \\ 1 & 0 & 0 \end{pmatrix}. \quad (5)$$

The group  $A_4$  has four irreducible representations, one triplet  $\mathbf{3}$  and three singlets  $\mathbf{1}$ ,  $\mathbf{1}'$ ,  $\mathbf{1}''$  with the multiplication rules  $\mathbf{3} \otimes \mathbf{3} = \mathbf{3}_s \oplus \mathbf{3}_a \oplus \mathbf{1} \oplus \mathbf{1}' \oplus \mathbf{1}''$ ,  $\mathbf{1}' \otimes \mathbf{1}'' = \mathbf{1}$ ,  $\mathbf{1}' \otimes \mathbf{1}' = \mathbf{1}''$ , and  $\mathbf{1}'' \otimes \mathbf{1}'' = \mathbf{1}'$ . Let us denote two  $A_4$  triplets as  $(a_1, a_2, a_3)$  and  $(b_1, b_2, b_3)$ ; then we have

$$\begin{aligned} (a \otimes b)_{\mathbf{3}_s} &= (a_2 b_3 + a_3 b_2, a_3 b_1 + a_1 b_3, a_1 b_2 + a_2 b_1), \\ (a \otimes b)_{\mathbf{3}_a} &= (a_2 b_3 - a_3 b_2, a_3 b_1 - a_1 b_3, a_1 b_2 - a_2 b_1), \\ (a \otimes b)_{\mathbf{1}} &= a_1 b_1 + a_2 b_2 + a_3 b_3, \\ (a \otimes b)_{\mathbf{1}'} &= a_1 b_1 + \omega a_2 b_2 + \omega^2 a_3 b_3, \\ (a \otimes b)_{\mathbf{1}''} &= a_1 b_1 + \omega^2 a_2 b_2 + \omega a_3 b_3, \end{aligned} \quad (6)$$

where  $\omega = e^{i2\pi/3}$  is a complex cubic root of unity. The representations of the field content of the model under  $SU(2) \times U(1) \times A_4 \times Z_2$  are summarized in Table I.

With the field content and the symmetries specified in Table I, the relevant renormalizable Lagrangian for the neutrino and charged lepton sectors invariant under  $SU(2) \times U(1) \times A_4 \times Z_2$  is given by

$$\begin{aligned} -\mathcal{L}_{\text{Yuk}} &= y_1^{\nu} \bar{L}_e (\tilde{\eta} N_R)_{\mathbf{1}} + y_2^{\nu} \bar{L}_{\mu} (\tilde{\eta} N_R)_{\mathbf{1}'} + y_3^{\nu} \bar{L}_{\tau} (\tilde{\eta} N_R)_{\mathbf{1}''} \\ &+ \frac{M}{2} (\bar{N}_R^c N_R)_{\mathbf{1}} + \frac{\lambda \chi}{2} (\bar{N}_R^c N_R)_{\mathbf{3}_s} \chi + y_e \bar{L}_e \Phi l_R \\ &+ y_{\mu} \bar{L}_{\mu} \Phi l_R' + y_{\tau} \bar{L}_{\tau} \Phi l_R'' + \text{H.c.} \end{aligned} \quad (7)$$

where  $\tilde{\eta} \equiv i\tau_2 \eta^*$  with the Pauli matrix  $\tau_2$ . Here,  $L_{e,\nu,\tau}$  and  $l_R^{(i)}$  denote left-handed lepton  $SU(2)_L$  doublets and right-handed lepton  $SU(2)_L$  singlets, respectively. The higher dimensional operators ( $d \geq 5$ ) driven by  $\chi$  and  $\eta$  fields are suppressed by a cutoff scale  $\Lambda$  which is a very high energy scale. Thus, their contributions are expected to be very small and we do not include them in this work. In the above Lagrangian, mass terms of the charged leptons are given by the diagonal form because the Higgs scalar  $\Phi$  and the charged lepton fields are assigned to be  $A_4$  singlet. The heavy neutrinos  $N_{Ri}$  acquire a bare mass  $M$  as well as a mass induced by a vacuum of electroweak singlet scalar  $\chi$  assigned to be  $A_4$  triplet. While the standard Higgs scalar  $\Phi^0$  gets a VEV  $v = (2\sqrt{2}G_F)^{-1/2} = 174$  GeV, the neutral component of scalar doublet  $\eta$  would not acquire a non-trivial VEV because  $\eta$  has odd parity of  $Z_2$  as assigned in

TABLE I. Representations of the fields under  $A_4 \times Z_2$  and  $SU(2)_L \times U(1)_Y$ .

Field	$L_e, L_{\mu}, L_{\tau}$	$l_R, l_R', l_R''$	$N_R$	$\chi$	$\Phi$	$\eta$
$A_4$	$\mathbf{1}, \mathbf{1}', \mathbf{1}''$	$\mathbf{1}, \mathbf{1}', \mathbf{1}''$	$\mathbf{3}$	$\mathbf{3}$	$\mathbf{1}$	$\mathbf{3}$
$Z_2$	+	+	-	+	+	-
$SU(2)_L \times U(1)_Y$	$(2, -1)$	$(1, -2)$	$(1, 0)$	$(1, 0)$	$(2, 1)$	$(2, 1)$

Table I and the auxiliary  $Z_2$  symmetry is exactly conserved even after electroweak symmetry breaking:

$$\langle \eta_i^0 \rangle = 0, \quad (i = 1, 2, 3), \quad \langle \Phi^0 \rangle = v \neq 0. \quad (8)$$

Therefore, the neutral component of scalar doublet  $\eta$  can be a good dark matter candidate, and the usual seesaw mechanism does not operate because the neutrino Yukawa interactions cannot generate masses. However, the light Majorana neutrino mass matrix can be generated radiatively through one-loop with the help of the Yukawa interaction  $\bar{L}_L N_R \tilde{\eta}$  in the Lagrangian, which will be discussed

more in detail in Sec. III. In our model, the  $A_4$  flavor symmetry is spontaneously broken by  $A_4$  triplet scalars  $\chi$ . From the condition of the global minima of the scalar potential, we can obtain a vacuum alignment of the fields  $\chi$  relevant to achieving our goal.

The most general renormalizable scalar potential of  $\Phi$ ,  $\eta$ , and  $\chi$  invariant under  $SU(2)_L \times U(1)_Y \times A_4 \times Z_2$  is given as

$$V = V(\eta) + V(\Phi) + V(\chi) + V(\eta\Phi) + V(\eta\chi) + V(\Phi\chi), \quad (9)$$

where

$$\begin{aligned} V(\eta) &= \mu_\eta^2 (\eta^\dagger \eta)_1 + \lambda_1^\eta (\eta^\dagger \eta)_1 (\eta^\dagger \eta)_1 + \lambda_2^\eta (\eta^\dagger \eta)_{1'} (\eta^\dagger \eta)_{1''} + \lambda_3^\eta (\eta^\dagger \eta)_{3_s} (\eta^\dagger \eta)_{3_s} + \lambda_4^\eta (\eta^\dagger \eta)_{3_a} (\eta^\dagger \eta)_{3_a} \\ &\quad + \{\lambda_5^\eta (\eta^\dagger \eta)_{3_s} (\eta^\dagger \eta)_{3_a} + \text{H.c.}\}, \\ V(\Phi) &= \mu_\Phi^2 (\Phi^\dagger \Phi) + \lambda^\Phi (\Phi^\dagger \Phi)^2, \\ V(\chi) &= \mu_\chi^2 (\chi\chi)_1 + \lambda_1^\chi (\chi\chi)_1 (\chi\chi)_1 + \lambda_2^\chi (\chi\chi)_{1'} (\chi\chi)_{1''} + \lambda_3^\chi (\chi\chi)_{3_s} (\chi\chi)_{3_s} + \lambda_4^\chi (\chi\chi)_{3_a} (\chi\chi)_{3_a} \\ &\quad + \lambda_5^\chi (\chi\chi)_{3_s} (\chi\chi)_{3_a} + \xi_1^\chi \chi (\chi\chi)_{3_s} + \xi_2^\chi \chi (\chi\chi)_{3_a}, \\ V(\eta\Phi) &= \lambda_1^{\eta\Phi} (\eta^\dagger \eta)_1 (\Phi^\dagger \Phi) + \lambda_2^{\eta\Phi} (\eta^\dagger \Phi) (\Phi^\dagger \eta) + \{\lambda_3^{\eta\Phi} (\eta^\dagger \Phi) (\eta^\dagger \Phi) + \text{H.c.}\} \\ V(\eta\chi) &= \lambda_1^{\eta\chi} (\eta^\dagger \eta)_1 (\chi\chi)_1 + \lambda_2^{\eta\chi} (\eta^\dagger \eta)_{1'} (\chi\chi)_{1''} + \lambda_2^{\eta\chi*} (\eta^\dagger \eta)_{1''} (\chi\chi)_{1'} + \lambda_3^{\eta\chi} (\eta^\dagger \eta)_{3_s} (\chi\chi)_{3_s} (\chi\chi)_{3_s} \\ &\quad + \lambda_4^{\eta\chi} (\eta^\dagger \eta)_{3_s} (\chi\chi)_{3_a} + \lambda_5^{\eta\chi} (\eta^\dagger \eta)_{3_a} (\chi\chi)_{3_a} + \xi_1^{\eta\chi} (\eta^\dagger \eta)_{3_s} \chi V(\Phi\chi) \\ &= \lambda^{\Phi\chi} (\Phi^\dagger \Phi) (\chi\chi)_1. \end{aligned} \quad (10)$$

Here,  $\mu_\eta$ ,  $\mu_\Phi$ ,  $\mu_\chi$ ,  $\xi_1^\chi$ ,  $\xi_2^\chi$ ,  $\xi_1^{\eta\chi}$ , and  $\xi_2^{\eta\chi}$  have a mass dimension, whereas  $\lambda_{1,\dots,5}^\eta$ ,  $\lambda^\Phi$ ,  $\lambda_{1,\dots,5}^\chi$ ,  $\lambda_{1,\dots,3}^{\eta\Phi}$ ,  $\lambda_{1,\dots,6}^{\eta\chi}$ , and  $\lambda^{\Phi\chi}$  are all dimensionless. In  $V(\eta\Phi)$ , the usual mixing terms  $\Phi^\dagger \eta$  and  $\Phi^\dagger \eta\chi$  are forbidden by the  $A_4 \times Z_2$  symmetry. The vacuum configuration is obtained by vanishing of the derivative of  $V$  with respect to each component of the scalar fields  $\Phi$  and  $\chi_i$  but with  $\langle \eta_i \rangle = 0$  ( $i = 1, 2, 3$ ), as follows:

$$\begin{aligned} \frac{\partial V}{\partial \chi_1} \Big|_{\langle \chi_i \rangle = v_{\chi_i}} &= 2v_{\chi_1} \{v_\Phi^2 \lambda^{\Phi\chi} + \mu_\chi^2 + (2\lambda_1^\chi - \lambda_2^\chi + 4\lambda_3^\chi)(v_{\chi_2}^2 + v_{\chi_3}^2) + 2(\lambda_1^\chi + \lambda_2^\chi)v_{\chi_1}^2\} + 6\xi_1^\chi v_{\chi_2} v_{\chi_3} = 0, \\ \frac{\partial V}{\partial \chi_2} \Big|_{\langle \chi_i \rangle = v_{\chi_i}} &= 2v_{\chi_2} \{v_\Phi^2 \lambda^{\Phi\chi} + \mu_\chi^2 + (2\lambda_1^\chi - \lambda_2^\chi + 4\lambda_3^\chi)(v_{\chi_1}^2 + v_{\chi_3}^2) + 2(\lambda_1^\chi + \lambda_2^\chi)v_{\chi_2}^2\} + 6\xi_1^\chi v_{\chi_1} v_{\chi_3} = 0, \\ \frac{\partial V}{\partial \chi_3} \Big|_{\langle \chi_i \rangle = v_{\chi_i}} &= 2v_{\chi_3} \{v_\Phi^2 \lambda^{\Phi\chi} + \mu_\chi^2 + (2\lambda_1^\chi - \lambda_2^\chi + 4\lambda_3^\chi)(v_{\chi_1}^2 + v_{\chi_2}^2) + 2(\lambda_1^\chi + \lambda_2^\chi)v_{\chi_3}^2\} + 6\xi_1^\chi v_{\chi_1} v_{\chi_2} = 0. \end{aligned} \quad (11)$$

From those equations, we can get<sup>2</sup>

$$\begin{aligned} \langle \chi_1 \rangle \equiv v_\chi &= \sqrt{\frac{-\mu_\chi^2 - v_\Phi^2 \lambda^{\Phi\chi}}{2(\lambda_1^\chi + \lambda_2^\chi)}} \neq 0, \\ \langle \chi_2 \rangle &= \langle \chi_3 \rangle = 0, \end{aligned} \quad (12)$$

<sup>2</sup>There exists another nontrivial solution  $\langle \chi \rangle = v_\chi(1, 1, 1)$  with  $v_\chi = \frac{-3\xi_1^\chi \pm \sqrt{9\xi_1^{\chi 2} - 8(\mu_\chi^2 + v_\Phi^2 \lambda^{\Phi\chi})(3\lambda_1^\chi + 4\lambda_3^\chi)}}{4(3\lambda_1^\chi + 4\lambda_3^\chi)}$ . However, it is not desirable for our purpose.

where  $v_\chi$  is real. Requiring vanishing of the derivative of  $V$  with respect to  $\Phi$ ,

$$\begin{aligned} \frac{\partial V}{\partial \varphi^0} \Big|_{\langle \varphi^0 \rangle = v_\Phi} &= 2v_\Phi \{2v_\Phi^2 \lambda^\Phi + \mu_\Phi^2 \\ &\quad + \lambda^{\Phi\chi}(v_{\chi_1}^2 + v_{\chi_2}^2 + v_{\chi_3}^2)\} = 0, \end{aligned} \quad (13)$$

and inserting the results given by Eq. (12), we obtain electroweak VEV,

$$v \equiv v_\Phi = \sqrt{\frac{-\mu_\Phi^2 - v_\chi^2 \lambda^{\Phi\chi}}{2\lambda^\Phi}}. \quad (14)$$

In our scenario, we assume that  $v_\chi$  is larger than  $v_\Phi$ .

After the breaking of the flavor and electroweak symmetries, the vacuum alignment in Eq. (12) leads to the right-handed Majorana neutrino mass matrix expressed as

$$M_R = M \begin{pmatrix} 1 & 0 & 0 \\ 0 & 1 & \kappa e^{i\xi} \\ 0 & \kappa e^{i\xi} & 1 \end{pmatrix}, \quad (15)$$

where  $\kappa = |\lambda_\chi^s v_\chi / M|$ . In addition, the charged lepton sector has a diagonal mass matrix  $m_\ell = v \text{Diag}(y_e, y_\mu, y_\tau)$ . We note that the vacuum alignment in Eq. (12) implies that the  $A_4$  symmetry is spontaneously broken to its residual symmetry  $Z_2$  in the heavy neutrino sector since  $(1, 0, 0)$  is invariant under the generator  $S$  in Eq. (5).

After the scalar fields get VEVs, the Yukawa interactions in Eq. (7) and the charged gauge interactions in a weak eigenstate basis can be written as

$$-\mathcal{L} = \frac{1}{2} \bar{N}_R^c M_R N_R + \bar{\ell}_L m_\ell \ell_R + \bar{\nu}_L Y_\nu \hat{\eta} N_R + \frac{g}{\sqrt{2}} W_\mu^- \bar{\ell}_L \gamma^\mu \nu_L + \text{H.c.}, \quad (16)$$

where  $\hat{\eta} = \text{Diag}(\tilde{\eta}_1, \tilde{\eta}_2, \tilde{\eta}_3)$ . One can easily see that the neutrino Yukawa matrix is given as follows:

$$Y_\nu = \sqrt{3} \begin{pmatrix} y_1^\nu & 0 & 0 \\ 0 & y_2^\nu & 0 \\ 0 & 0 & y_3^\nu \end{pmatrix} U_\omega^\dagger, \quad \text{with} \quad (17)$$

$$U_\omega = \frac{1}{\sqrt{3}} \begin{pmatrix} 1 & 1 & 1 \\ 1 & \omega^2 & \omega \\ 1 & \omega & \omega^2 \end{pmatrix}.$$

For our convenience, let us take the basis where heavy Majorana neutrino and charged lepton mass matrices are diagonal. Rotating the basis

$$N_R \rightarrow U_R^\dagger N_R, \quad (18)$$

$$U_{\text{PMNS}} = \begin{pmatrix} c_{13}c_{12} & & & \\ -c_{23}s_{12} - s_{23}c_{12}s_{13}e^{i\delta_{CP}} & c_{13}s_{12} & s_{13}e^{-i\delta_{CP}} & \\ s_{23}s_{12} - c_{23}c_{12}s_{13}e^{i\delta_{CP}} & c_{23}c_{12} - s_{23}s_{12}s_{13}e^{i\delta_{CP}} & s_{23}c_{13} & \\ -s_{23}c_{12} - c_{23}s_{12}s_{13}e^{i\delta_{CP}} & -s_{23}c_{12} - c_{23}s_{12}s_{13}e^{i\delta_{CP}} & c_{23}c_{13} & \end{pmatrix} Q_\nu, \quad (23)$$

where  $s_{ij} \equiv \sin\theta_{ij}$  and  $c_{ij} \equiv \cos\theta_{ij}$ , and  $Q_\nu = \text{Diag}(e^{-i\varphi_1/2}, e^{-i\varphi_2/2}, 1)$ . Here, we notice that the origin of the  $CP$  phases in  $U_{\text{PMNS}}$  is the  $CP$  phases  $\psi_1, \psi_2$  (or  $\xi$ ) originally coming from  $M_R$ , as can be seen by comparing

the right-handed Majorana mass matrix  $M_R$  becomes real and diagonal by a unitary matrix  $U_R$ ,

$$\hat{M}_R = U_R^T M_R U_R = M \text{Diag}(a, 1, b), \quad (19)$$

where  $a = \sqrt{1 + \kappa^2 + 2\kappa \cos\xi}$  and  $b = \sqrt{1 + \kappa^2 - 2\kappa \cos\xi}$  with real and positive mass eigenvalues,  $M_1 = Ma$ ,  $M_2 = M$ , and  $M_3 = Mb$ . The unitary matrix  $U_R$  diagonalizing  $M_R$  given in Eq. (15) is

$$U_R = \frac{1}{\sqrt{2}} \begin{pmatrix} 0 & \sqrt{2} & 0 \\ 1 & 0 & -1 \\ 1 & 0 & 1 \end{pmatrix} \begin{pmatrix} e^{i\frac{\psi_1}{2}} & 0 & 0 \\ 0 & 1 & 0 \\ 0 & 0 & e^{i\frac{\psi_2}{2}} \end{pmatrix}, \quad (20)$$

with the phases

$$\psi_1 = \tan^{-1}\left(\frac{-\kappa \sin\xi}{1 + \kappa \cos\xi}\right) \quad \text{and} \quad (21)$$

$$\psi_2 = \tan^{-1}\left(\frac{\kappa \sin\xi}{1 - \kappa \cos\xi}\right).$$

The phases  $\psi_{1,2}$  go to 0 or  $\pi$  as the magnitude of  $\kappa$  defined in Eq. (15) decreases. Due to the rotation (18), the neutrino Yukawa matrix  $Y_\nu$  gets modified to

$$\tilde{Y}_\nu = Y_\nu U_R = P_\nu^\dagger \text{Diag}(|y_1^\nu|, |y_2^\nu|, |y_3^\nu|) U_\omega^\dagger U_R. \quad (22)$$

Absorbing  $P_\nu$  into the neutrino field  $\nu_L$  and then transforming  $\ell_L \rightarrow P_\nu^* \ell_L$ ,  $\ell_R \rightarrow P_\nu^* \ell_R$ , we can make  $P_\nu$  disappear in  $\tilde{Y}_\nu$  as well as the Lagrangian Eq. (7). Then, the neutrino fields  $\nu_L$  in the weak basis are simply transformed into the mass basis by the lepton mixing matrix,  $U_{\text{PMNS}}$ , the so-called PMNS mixing matrix.

The lepton mixing matrix  $U_{\text{PMNS}}$  can be written in terms of three mixing angles and three  $CP$ -odd phases (one for the Dirac neutrino and two for the Majorana neutrino) as follows [10]:

Eqs. (15)–(22). Thus, we expect that there can be some correlation between low energy  $CP$  violation measurable from neutrino oscillations and high energy  $CP$  violation responsible for leptogenesis in the neutrino sector.

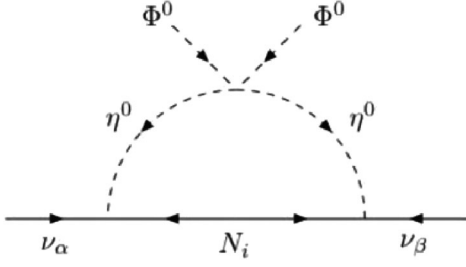


FIG. 1. One-loop generation of light neutrino masses.

### III. NEUTRINO MASSES AND MIXING ANGLES

We now proceed to investigate the low energy neutrino observables. Due to the auxiliary  $Z_2$  symmetry, the usual seesaw mechanism does not operate any more, and thus light neutrino masses cannot be generated at tree level. However, similar to the scenario presented in Ref. [8], the light neutrino mass matrix can be generated through the one-loop diagram drawn in Fig. 1 thanks to the quartic scalar interactions. After electroweak symmetry breaking, the light neutrino masses in the flavor basis where the charged lepton mass matrix is real and diagonal are written as

$$(m_\nu)_{\alpha\beta} = \sum_i \frac{\Delta m_{\eta_i}^2}{16\pi^2} \frac{(\tilde{Y}_\nu)_{\alpha i} (\tilde{Y}_\nu)_{\beta i}}{M_i} f\left(\frac{M_i^2}{\tilde{m}_{\eta_i}^2}\right), \quad (24)$$

where

$$f(z_i) = \frac{z_i}{1-z_i} \left[ 1 + \frac{z_i \ln z_i}{1-z_i} \right], \quad (25)$$

$$\Delta m_{\eta_i}^2 \equiv |m_{R_i}^2 - m_{I_i}^2| = 4v^2 \lambda_3^{\Phi\eta},$$

with  $z_i = M_i^2/\tilde{m}_{\eta_i}^2$ . The explicit expressions for  $\tilde{m}_{\eta_i}^2$  are presented in the Appendix. Here,  $m_{R_i}(m_{I_i})$  is the mass of the field component  $\eta_{R_i}^0(\eta_{I_i}^0)$  and  $m_{R_i(I_i)}^2 = \tilde{m}_{\eta_i}^2 \pm \Delta m_{\eta_i}^2/2$ , where the subscripts  $R$  and  $I$  indicate real and imaginary components, respectively. With  $\tilde{M}_R = \text{Diag}(M_{r1}, M_{r2}, M_{r3})$  and  $M_{ri} \equiv M_i f^{-1}(z_i)$ , the above formula Eq. (24) can be expressed as

$$m_\nu = \frac{v^2 \lambda_3^{\Phi\eta}}{4\pi^2} \tilde{Y}_\nu \tilde{M}_R^{-1} \tilde{Y}_\nu^T$$

$$= U_{\text{PMNS}} \text{Diag}(m_1, m_2, m_3) U_{\text{PMNS}}^T \quad (26)$$

$$= m_0 \begin{pmatrix} Ay_1^2 & By_1 y_2 & By_1 \\ By_1 y_2 & Dy_2^2 & Gy_2 \\ By_1 & Gy_2 & D \end{pmatrix},$$

where  $m_i$  ( $i = 1, 2, 3$ ) are the light neutrino mass eigenvalues,  $y_{1(2)} = y_{1(2)}^\nu/y_3^\nu$ , and

$$A = f(z_2) + \frac{2e^{i\psi_1} f(z_1)}{a}, \quad B = f(z_2) - \frac{e^{i\psi_1} f(z_1)}{a},$$

$$D = f(z_2) + \frac{e^{i\psi_1} f(z_1)}{2a} - \frac{3e^{i\psi_2} f(z_3)}{2b}, \quad m_0 = \frac{v^2 |y_3^\nu|^2 \lambda_3^{\Phi\eta}}{4\pi^2 M},$$

$$G = f(z_2) + \frac{e^{i\psi_1} f(z_1)}{2a} + \frac{3e^{i\psi_2} f(z_3)}{2b}. \quad (27)$$

It is worthwhile to notice that in the limit of  $y_2 \rightarrow 1$  the above mass matrix in Eq. (26) goes to  $\mu - \tau$  symmetry, leading to  $\theta_{13} = 0$  and  $\theta_{23} = -\pi/4$ . Moreover, in the limit of  $y_1, y_2 \rightarrow 1$  the above mass matrix gives TBM angles and mass eigenvalues, respectively,

$$\theta_{13} = 0, \quad \theta_{23} = -\frac{\pi}{4}, \quad \theta_{12} = \sin^{-1}\left(\frac{1}{\sqrt{3}}\right),$$

$$m_1 = 3m_0 \frac{f(z_1)}{a} e^{i\psi_1}, \quad m_2 = 3m_0 f(z_2), \quad (28)$$

$$m_3 = 3m_0 \frac{f(z_3)}{b} e^{i(\psi_2 + \pi)},$$

indicating that mass eigenvalues are divorced from mixing angles. However, recent neutrino data, including the observations of nonzero  $\theta_{13}$ , requires deviations of  $y_{1,2}$  from unit.

Now, let us show how deviations of  $y_{1,2}$  from unit are responsible for nonvanishing  $\theta_{13}$  and how they are related to neutrino mass eigenvalues. To separately obtain real values for the neutrino mixing angles and masses, we diagonalize the Hermitian matrix  $m_\nu m_\nu^\dagger$  with  $m_\nu$  given by Eq. (26),

$$m_\nu m_\nu^\dagger = m_0^2 \begin{pmatrix} \tilde{A} y_1^2 & y_1 y_2 \left( \frac{P-Q}{2} - i \frac{3(R+S)}{2} \right) & y_1 \left( \frac{P+Q}{2} - i \frac{3(R-S)}{2} \right) \\ y_1 y_2 \left( \frac{P-Q}{2} + i \frac{3(R+S)}{2} \right) & y_2^2 \frac{\tilde{F} + \tilde{G} - \tilde{K}}{4} & y_2 \left( \frac{\tilde{F} - \tilde{G}}{4} - i \frac{3\tilde{D}}{2} \right) \\ y_1 \left( \frac{P+Q}{2} + i \frac{3(R-S)}{2} \right) & y_2 \left( \frac{\tilde{F} - \tilde{G}}{4} + i \frac{3\tilde{D}}{2} \right) & \frac{\tilde{F} + \tilde{G} - \tilde{K}}{4} \end{pmatrix}$$

$$= U_{\text{PMNS}} \text{Diag}(m_1^2, m_2^2, m_3^2) U_{\text{PMNS}}^\dagger, \quad (29)$$

where  $\tilde{A}, \tilde{D}, \tilde{F}, \tilde{G}, \tilde{K}, P, Q, R$ , and  $S$  are real:

$$\begin{aligned}
\tilde{A} &= (1 + 4y_1^2 + y_2^2) \frac{f^2(z_1)}{a^2} + (1 + y_1^2 + y_2^2) f^2(z_2) - 2(1 - 2y_1^2 + y_2^2) \frac{f(z_1)f(z_2)}{a} \cos\psi_1, \\
\tilde{F} &= (1 + 4y_1^2 + y_2^2) \frac{f^2(z_1)}{a^2} + 4(1 + y_1^2 + y_2^2) f^2(z_2) + 4(1 - 2y_1^2 + y_2^2) \frac{f(z_1)f(z_2)}{a} \cos\psi_1, \\
\tilde{K} &= 6(1 - y_2^2) \frac{f(z_3)}{b} \left( \frac{f(z_1)}{a} \cos\psi_{12} + 2f(z_2) \cos\psi_2 \right), \\
\tilde{G} &= 9(1 + y_2^2) \frac{f^2(z_3)}{b^2}, \\
\tilde{D} &= (1 - y_2^2) \frac{f(z_3)}{b} \left( \frac{f(z_1)}{a} \sin\psi_{12} - 2f(z_2) \sin\psi_2 \right), \\
P &= -(1 + 4y_1^2 + y_2^2) \frac{f^2(z_1)}{a^2} + 2(1 + y_1^2 + y_2^2) f^2(z_2) - (1 - 2y_1^2 + y_2^2) \frac{f(z_1)f(z_2)}{a} \cos\psi_1, \\
Q &= 3(1 - y_2^2) \frac{f(z_3)}{b} \left( \frac{f(z_1)}{a} \cos\psi_{12} - f(z_2) \cos\psi_2 \right), \\
R &= (1 - 2y_1^2 + y_2^2) \frac{f(z_1)f(z_2)}{a} \sin\psi_1, \\
S &= (1 - y_2^2) \frac{f(z_3)}{b} \left( \frac{f(z_1)}{a} \sin\psi_{12} + f(z_2) \sin\psi_2 \right),
\end{aligned} \tag{30}$$

with  $\psi_{ij} \equiv \psi_i - \psi_j$ . To see how the neutrino mass matrix given by Eq. (26) can lead to the deviations of neutrino mixing angles from their TBM values, we first introduce three small quantities  $\epsilon_i$ , ( $i = 1-3$ ), which are responsible for the deviations of the  $\theta_{jk}$  from their TBM values:

$$\theta_{23} = -\frac{\pi}{4} + \epsilon_1, \quad \theta_{13} = \epsilon_2, \quad \theta_{12} = \sin^{-1}\left(\frac{1}{\sqrt{3}}\right) + \epsilon_3. \tag{31}$$

Then, the PMNS mixing matrix keeping unitarity up to order of  $\epsilon_i$  can be written as

$$U_{\text{PMNS}} = \begin{pmatrix} \frac{\sqrt{2}-\epsilon_3}{\sqrt{3}} & \frac{1+\epsilon_3\sqrt{2}}{\sqrt{3}} & \epsilon_2 e^{-i\delta_{CP}} \\ -\frac{1+\epsilon_1+\epsilon_3\sqrt{2}}{\sqrt{6}} + \frac{\epsilon_2 e^{i\delta_{CP}}}{\sqrt{3}} & \frac{\sqrt{2}+\epsilon_1\sqrt{2}-\epsilon_3}{\sqrt{6}} + \frac{\epsilon_2 e^{i\delta_{CP}}}{\sqrt{6}} & \frac{-1+\epsilon_1}{\sqrt{2}} \\ \frac{-1+\epsilon_1+\epsilon_3\sqrt{2}}{\sqrt{6}} - \frac{\epsilon_2 e^{i\delta_{CP}}}{\sqrt{3}} & \frac{\sqrt{2}-\epsilon_3-\sqrt{2}\epsilon_1}{\sqrt{6}} - \frac{\epsilon_2 e^{i\delta_{CP}}}{\sqrt{6}} & \frac{1+\epsilon_1}{\sqrt{2}} \end{pmatrix} Q_\nu + \mathcal{O}(\epsilon_i^2). \tag{32}$$

The small deviation  $\epsilon_1$  from maximality of the atmospheric mixing angle is expressed in terms of the parameters in Eq. (30) as

$$\tan\epsilon_1 = \frac{R(1+y_2) - S(1-y_2)}{R(1-y_2) - S(1+y_2)}. \tag{33}$$

The reactor angle  $\theta_{13}$  and Dirac-CP phase  $\delta_{CP}$  are expressed as

$$\begin{aligned}
\tan 2\theta_{13} &\simeq \frac{y_1 |\Omega|}{\sqrt{2}(\Theta - \tilde{A})}, \\
\tan \delta_{CP} &= 3 \frac{(R-S)^2 + y_2^2(R+S)^2}{(P+Q)(R-S) - y_2^2(P-Q)(R+S)},
\end{aligned} \tag{34}$$

where

$$\begin{aligned}
\Omega &= (1-y_2)P + (1+y_2)Q + \epsilon_1\{(1+y_2)P \\
&\quad + (1-y_2)Q - 3i\{R(1-y_2) - S(1+y_2) \\
&\quad + \epsilon_1(R(1+y_2) - S(1-y_2))\}, \\
\Theta &= \frac{1}{4} \left\{ (\tilde{F} + \tilde{G} - \tilde{K}) \left( \frac{1+y_2^2}{2} + \epsilon_1(1-y_2^2) \right) \right. \\
&\quad \left. - y_2(\tilde{F} - \tilde{G}) \right\}.
\end{aligned} \tag{35}$$

In the limit of  $y_1, y_2 \rightarrow 1$ , the parameters  $Q, R, S, \epsilon_1$  go to zero, which in turn leads to  $\theta_{13} \rightarrow 0$  and  $\delta_{CP} \rightarrow 0$  as expected. Finally, the solar mixing angle is given as

$$\tan 2\theta_{12} \simeq \frac{y_1 Z}{\sqrt{2}(\Psi_2 - \Psi_1)}, \quad (36)$$

where the parameters  $\Psi_1$ ,  $\Psi_2$ , and  $Z$  with  $|\epsilon_i| \ll 1$  are given as

$$\begin{aligned} \Psi_1 &\simeq \tilde{A} - \frac{\epsilon_2 |\Omega|}{\sqrt{2}}, \\ Z &\simeq P(1 + y_2) + Q(1 - y_2) - \epsilon_1 \{P(1 - y_2) \\ &\quad + Q(1 + y_2)\}, \\ \Psi_2 &\simeq \frac{\tilde{F} + \tilde{G} - \tilde{K}}{8} (1 + y_2^2) + \frac{\tilde{F} - \tilde{G}}{4} y_2 \\ &\quad - \epsilon_1 \frac{\tilde{F} + \tilde{G} - \tilde{K}}{4} (1 - y_2^2). \end{aligned} \quad (37)$$

Note that in Eq. (36) the condition  $P(1 + y_2) + Q(1 - y_2) \gg |\epsilon_1 \{P(1 - y_2) + Q(1 + y_2)\}|$  should be satisfied, in order for the solar mixing angle  $\theta_{12}$  to lie in the allowed region from the experimental data given in Eq. (3). The squared-mass eigenvalues of three light neutrinos are given by

$$\begin{aligned} m_1^2 &\simeq m_0^2 \left[ c_{12}^2 \Psi_1 + s_{12}^2 \Psi_2 - \frac{y_1 Z}{2\sqrt{2}} \sin 2\theta_{12} \right], \\ m_2^2 &\simeq m_0^2 \left[ s_{12}^2 \Psi_1 + c_{12}^2 \Psi_2 + \frac{y_1 Z}{2\sqrt{2}} \sin 2\theta_{12} \right], \\ m_3^2 &\simeq m_0^2 \left[ \Theta + \frac{\epsilon_2 |\Omega|}{\sqrt{2}} \right]. \end{aligned} \quad (38)$$

We see from Eq. (37) that the deviation  $\epsilon_3$  from trimaximality of the solar mixing angle is roughly expressed as

$$\sin \epsilon_3 \simeq \frac{y_1 3\sqrt{2} Z m_0^2}{2\Delta m_{21}^2} - 2\sqrt{2}. \quad (39)$$

In the limit of  $|\epsilon_i| \ll 1$ , the solar and atmospheric mass-squared differences are roughly given in a good approximation by

$$\begin{aligned} \Delta m_{\text{Sol}}^2 &\equiv m_2^2 - m_1^2 \\ &\simeq \frac{m_0^2}{24} \{ (\tilde{F} + \tilde{G} - \tilde{K})(1 + y_2^2) + 2y_2(\tilde{F} - \tilde{G}) \\ &\quad - 8\tilde{A} + 16y_1(P(1 + y_2) + Q(1 - y_2)) \}, \\ \Delta m_{\text{Atm}}^2 &\equiv m_3^2 - m_1^2 \\ &\simeq \frac{m_0^2}{3} \left\{ \frac{\tilde{F} + \tilde{G} - \tilde{K}}{4} (1 + y_2^2) - y_2(\tilde{F} - \tilde{G}) \right. \\ &\quad \left. - 2\tilde{A} - y_1(P(1 + y_2) + Q(1 - y_2)) \right\}. \end{aligned} \quad (40)$$

Here we note that the parameter  $M_{ri}$  in Eq. (26) can be simplified in the following limiting cases as

$$M_{ri} \simeq \begin{cases} M_i [\ln z_i - 1]^{-1}, & \text{for } z_i \gg 1 \\ 2M_i, & \text{for } z_i \rightarrow 1 \\ \bar{m}_\eta^2 M_i^{-1}, & \text{for } z_i \ll 1. \end{cases} \quad (41)$$

#### IV. NUMERICAL RESULTS

As is well known, the observed hierarchy  $|\Delta m_{\text{Atm}}^2| \gg \Delta m_{\text{Sol}}^2 > 0$  leads to two possible neutrino mass spectrum: (i)  $m_1 < m_2 < m_3$  (normal mass spectrum), and (ii)  $m_3 < m_1 < m_2$  (inverted mass spectrum). Since there are many unknown parameters such as masses of heavy Majorana neutrinos and scalar fields  $\eta_R$ ,  $\eta_I$ , we consider a particular parameter set for those parameters and show how the measured values of the mixing angle  $\theta_{13}$  can be accommodated in our model, while the other neutrino parameters such as solar and atmospheric mixing angles and mass-squared differences are satisfied with the current data.

The mass matrix in Eq. (26) contains 10 free parameters:  $\lambda_3^{\Phi\eta}$ ,  $M$ ,  $y_3^\nu$ ,  $z_1$ ,  $z_2$ ,  $z_3$  and  $y_1$ ,  $y_2$ ,  $\xi$ ,  $\kappa$ . The combination of the first three of them,  $\{\lambda_3^{\Phi\eta}, M, y_3^\nu\}$ , leads to the overall neutrino scale parameter  $m_0$ . As shown above, the elements of the mass matrix in Eq. (26) are expressed in terms of measurable neutrino parameters,  $\theta_{12}$ ,  $\theta_{13}$ ,  $\theta_{23}$ ,  $m_{1,2,3}$ ,  $\delta_{CP}$ ,  $\varphi_{1,2}$ . Among them, three mixing angles and two mass-squared differences are measured. For numerical analysis [11], we need to fix some parameters by hand since there are too many model parameters to be predicted. As an example, we take a case  $M_1^2 = \bar{m}_{\eta_1}^2$ ,  $M_2^2 = 1.3\bar{m}_{\eta_2}^2$ ,  $M_3^2 = 1.5\bar{m}_{\eta_3}^2$  and fix the overall seesaw scale  $M$  to be 1 TeV. Then, the parameters  $m_0$ ,  $y_1$ ,  $y_2$ ,  $\kappa$ ,  $\xi$  can be determined from the experimental results of three mixing angles and two mass-squared differences. In addition, the  $CP$  phases  $\delta_{CP}$ ,  $\varphi_{1,2}$  can be predicted after determining the model parameters. Depending on the values of the model parameters, there exist two possibilities for the light neutrino spectrum; one is normal mass hierarchy and the other is inverted hierarchy. In the following, we discuss the two cases separately.

##### A. Normal hierarchy of a light neutrino

Based on the formulas for the neutrino mixing angles and masses, we numerically scan the parameters  $m_0$ ,  $y_1$ ,  $y_2$ ,  $\kappa$ ,  $\xi$  and then pick up the values of those five parameters which are consistent with the experimental data given at  $3\sigma$  in Eq. (3). For the mixing angle  $\theta_{13}$ , we allow its value a bit widely from  $5$  to  $15^\circ$  instead of its experimental values at  $3\sigma$ .<sup>3</sup> In such a way, we can obtain the allowed regions of the parameters given by

<sup>3</sup>Note that a very small mixing angle  $\theta_{13}$  of less than  $1^\circ$  can be achieved in the case that  $y_1 \rightarrow 1$  or  $\sin \psi_1 \rightarrow 0$  converges more faster than  $y_2 \rightarrow 1$ .

$$\begin{aligned}
1.40 < \kappa < 2.38, \quad 0.44 < y_1 < 0.89, \\
0.60 < y_2 < 0.84 \quad \text{and} \quad 1.1 < y_2 < 1.89, \\
190^\circ \leq \xi < 211^\circ, \quad 0.23 \leq \frac{y_3^\nu \lambda_3^{\Phi_\eta}}{10^{-9}} < 0.46.
\end{aligned}
\tag{42}$$

We found that normal mass ordering of a light neutrino can be achieved when  $M_1 \lesssim M_2 < M_3$  or  $M_2 \lesssim M_1 < M_3$  are satisfied for the parameter spaces given above. In the upper left panel of Fig. 2, the data points indicate how the mixing angle  $\theta_{13}$  is determined in terms of the ratio  $y_1/y_2$ . The result shows that the upper limit of  $y_1/y_2$  is 0.86, and the measured value of  $\theta_{13}$  from Daya Bay and RENO can be achieved for two regions,  $0.40 < y_1/y_2 < 0.57$  and  $0.67 < y_1/y_2 < 0.82$ . To see how the parameters are correlated with low energy  $CP$  violation measurable through neutrino oscillations, we consider the leptonic  $CP$  violation parameter defined by the Jarlskog invariant  $J_{CP} \equiv \text{Im}[U_{e1}U_{\mu 2}U_{e2}^*U_{\mu 1}^*] = \frac{1}{8} \sin 2\theta_{12} \sin 2\theta_{23} \sin 2\theta_{13} \cos \theta_{13} \sin \delta_{CP}$  [12], which can be described in terms of the elements  $h = m_\nu m_\nu^\dagger$  [13]:

$$J_{CP} = -\frac{\text{Im}\{h_{12}h_{23}h_{31}\}}{\Delta m_{21}^2 \Delta m_{31}^2 \Delta m_{32}^2}.
\tag{43}$$

The behavior of  $J_{CP}$  is plotted in the upper right panel of Fig. 2 as a function of  $\theta_{13}$ . We see that the value of  $|J_{CP}|$  lies between 0 and 0.034 for the measured value of  $\theta_{13}$ . In our model, since  $\text{Im}\{h_{12}h_{23}h_{31}\}$  is proportional to  $1 - y_2^2$ , the leptonic  $CP$  violation  $J_{CP}$  goes to zero in the limit of  $y_2 \rightarrow 1$ . However,  $y_2 = 1$  is not allowed in our analysis, and thus  $J_{CP} = 0$  indicates that there exists some cancellation among the terms composed of  $\sin \psi_{12}$ ,  $\sin(\psi_1 + \psi_2)$ , and  $\sin(2\psi_1 - \psi_2)$ ;  $\sin \psi_2$  multiplies by  $y_{1,2}$ ,  $f(z_1)/a$ ,  $f(z_2)$ , and  $f(z_3)/b$  even if  $CP$  phases  $\psi_{1,2}$  are nonzero. In the lower panels of Fig. 2, the data points indicate how the values of  $\theta_{13}$  depend on  $\theta_{12}$  and  $\theta_{23}$  in the allowed regions given by Eq. (3). We see that the measured values of  $\theta_{13}$  can be achieved for two separate regions of  $\theta_{23}$ :  $38.6^\circ \leq \theta_{23} \leq 43^\circ$  and  $47^\circ \leq \theta_{23} \leq 53.1^\circ$ , which indicates that the parameter set strongly prefers deviations from maximal mixing for the atmospheric neutrino oscillation. From the

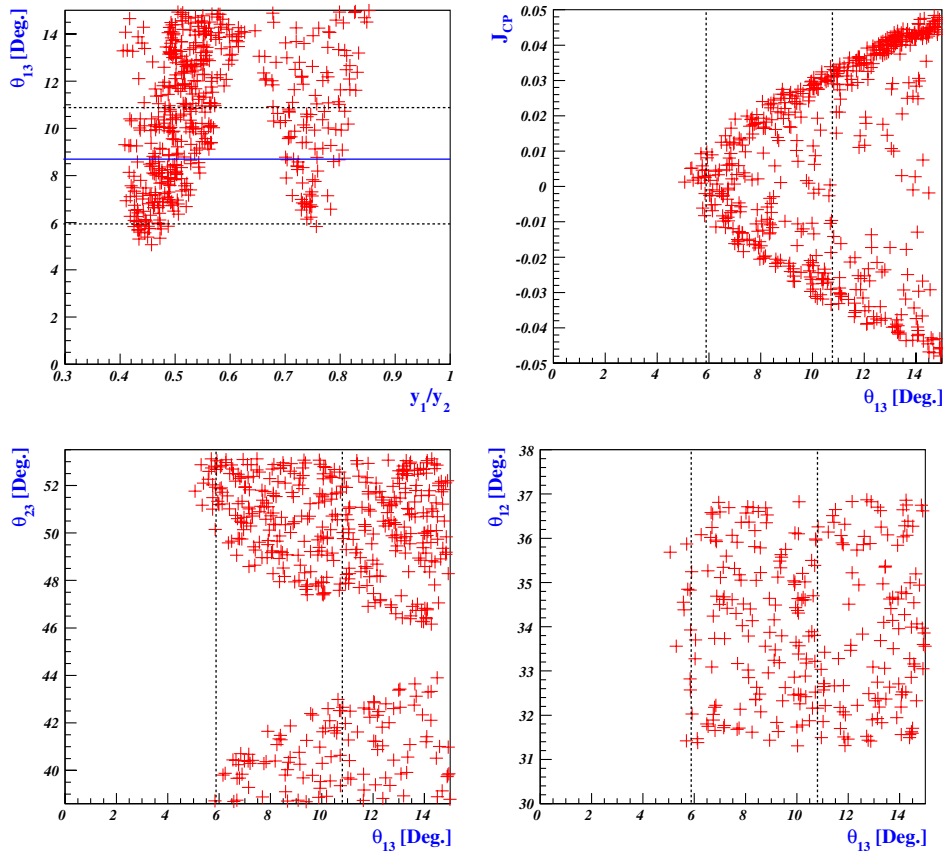


FIG. 2 (color online). Plots for case (i) displaying the reactor mixing angle  $\theta_{13}$  versus the ratio  $y_1/y_2$  (upper left panel), and the Jarlskog invariant  $J_{CP}$  versus the reactor angle  $\theta_{13}$  (upper right panel). Allowed values for the atmospheric mixing angle  $\theta_{23}$  (lower left panel) and the solar mixing angle  $\theta_{12}$  (lower right panel) versus the mixing angle  $\theta_{13}$ , respectively. The thick line corresponds to  $\theta_{13} = 8.68^\circ$ , which is the best-fit value of Eq. (2) including the Daya Bay result. The horizontal and vertical dotted lines in both plots indicate the upper and lower bounds on  $\theta_{13}$  given in Eq. (2) at  $3\sigma$ .



lower right panel of Fig. 2, we see that predictions of  $\theta_{13}$  do not strongly depend on  $\theta_{12}$  for the allowed region. We see from the figures that  $\theta_{13}$  for the normal hierarchy prefers rather large values greater than  $5^\circ$ .

We also see from Fig. 2 that small deviations of  $\theta_{23}$  prefer large values of  $\theta_{13}$  in the normal hierarchical case. This can be understood by considering two relations given

$$\tan \epsilon_1 = \frac{(1 + y_2)(1 - 2y_1^2 + y_2^2) \sin \psi_1 \frac{f(z_1)f(z_2)}{a} - (1 - y_2)^2 \frac{f(z_3)}{b} \left(\frac{f(z_1)}{a}\right) \sin \psi_{12} + f(z_2) \sin \psi_2}{(1 - y_2)(1 - 2y_1^2 + y_2^2) \sin \psi_1 \frac{f(z_1)f(z_2)}{a} - (1 + y_2)^2 \frac{f(z_3)}{b} \left(\frac{f(z_1)}{a}\right) \sin \psi_{12} + f(z_2) \sin \psi_2}.$$

This formula for the parameter  $\epsilon_1$  is relevant only when  $y_2 \neq 1$ . In the case of  $y_2 \rightarrow 1$  while  $y_1 \neq 1$  and  $\sin \psi_1 \neq 0$ , we see from the above equation that the value of  $\theta_{23}$  (or  $\epsilon_1$ ) can be large but restricted by experimental data. Then, due to Eq. (26) and  $\Omega$  in Eq. (35), the value of  $\theta_{13}$  gets smaller as  $y_2 \rightarrow 1$ . On the other hand, when  $y_2$  is much deviated from 1, two cases for  $\theta_{23}$  (or  $\epsilon_1$ ) are possible. One is that rather smaller values of  $\theta_{23}$  (or  $\epsilon_1$ ) are preferred as the value of  $\kappa$  (or  $\sin \psi_1 \rightarrow 0$  and  $\sin \psi_2 \rightarrow 0$ ) decreases, and the other is that the combination of two parts in the numerator of the above equation can lead to wide ranges of  $\theta_{23}$  (or  $\epsilon_1$ ). However, when  $y_2 \approx 1$ , which makes the above equation irrelevant, the value of  $\theta_{13}$  goes to  $0^\circ$  (numerically  $\lesssim 1^\circ$ ), and the value of  $\theta_{23}$  can approach  $45^\circ$  (or  $\epsilon_1 \rightarrow 0$ ) for  $y_1 \rightarrow 1$  or  $\sin \psi_1 \rightarrow 0$  converges faster than  $y_2 \rightarrow 1$ . We have neglected this case in our paper.

By using the conventional parametrization of the PMNS matrix [10] and Eq. (32), one can deduce an expression for the Dirac  $CP$  phase  $\delta_{CP}$  given by

$$\delta_{CP} = -\arg \left( \frac{U_{e1}^* U_{e3} U_{\tau 1} U_{\tau 3}^* + c_{12} c_{23} s_{13}}{s_{12} s_{23}} \right). \quad (44)$$

in Eqs. (21) and (26). The phases  $\psi_{1,2}$  go to 0 or  $\pi$  as the magnitude of  $\kappa$  defined in Eq. (15) decreases, and in the case of  $y_2 = 1$  the neutrino mass matrix indicates directly that  $\theta_{13} = 0$  and  $\theta_{23} = -\pi/4$ . However, deviation of  $y_2$  from one can be associated with deviation from maximality of the atmospheric mixing angle by the following relation:

Moreover, we can straightforwardly obtain the effective neutrino mass  $|m_{ee}|$ , which is associated with the amplitude for neutrinoless double beta decay:

$$|m_{ee}| \equiv \left| \sum_i (U_{PMNS})_{ei}^2 m_i \right|, \quad (45)$$

where  $U_{PMNS}$  is given in Eq. (32). The left panel of Fig. 3 shows that  $\delta_{CP}$  is predicted to be  $0^\circ \leq \delta_{CP} \leq 60^\circ$ ,  $120^\circ \leq \delta_{CP} \leq 240^\circ$ , and  $300^\circ \leq \delta_{CP} \leq 360^\circ$  for the measured values of  $\theta_{13}$  at  $3\sigma$ . In the right panel of Fig. 3, we plot the prediction of the effective neutrino mass  $|m_{ee}|$  as a function of  $\theta_{13}$ , which lies between 0.014 and 0.021 in the region of the measured values of  $\theta_{13}$  at  $3\sigma$ .

## B. Inverted hierarchy of a light neutrino

Now let us turn to the inverted hierarchical case. Similar to case (i), scanning the parameters  $m_0, y_1, y_2, \kappa, \xi$  based on the formulas for the neutrino mixing angles and masses and taking the experimental data given at  $3\sigma$  in Eq. (3) as constraints, we can obtain the allowed regions of model parameters given by

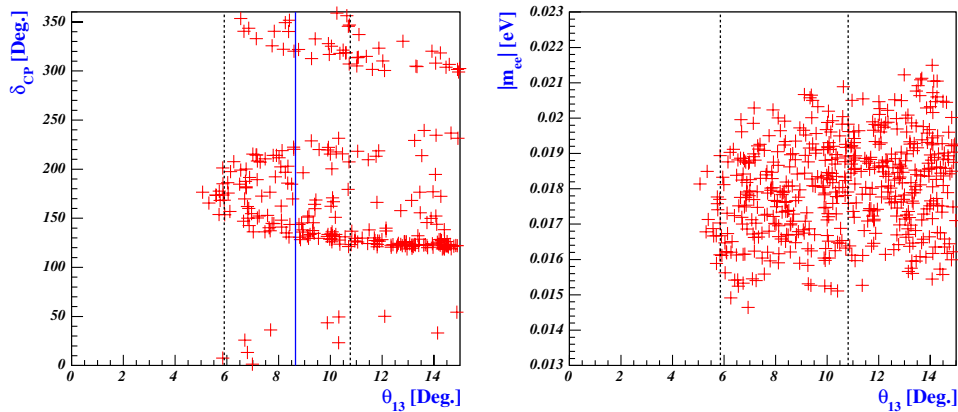


FIG. 3 (color online). Predictions for the Dirac  $CP$  phase  $\delta_{CP}$  versus  $\theta_{13}$  (left panel) and the effective mass of neutrinoless double beta decay  $|m_{ee}|$  versus the mixing angle  $\theta_{13}$  (right panel) for Case (i). The thick and dotted lines correspond to  $\theta_{13} = 8.68^\circ$  which is the best-fit value and the  $3\sigma$  bounds given in Eq. (2) including the Daya Bay result, respectively.

$$\begin{aligned}
 &1.30 < \kappa < 1.56, \quad 209^\circ \leq \xi < 222^\circ, \\
 &0.27 \leq \frac{y_3^\nu \lambda_3^{\Phi\eta}}{10^{-9}} < 0.45, \quad 0.79 < y_1 < 0.88, \\
 &0.60 < y_2 < 0.79, \quad \text{and} \quad 1.12 < y_1 < 1.24, \\
 &1.28 < y_2 < 1.5.
 \end{aligned}
 \tag{46}$$

We found that this case is achieved when  $M_1 < M_2 < M_3$  is satisfied. For those parameter regions, we in turn investigate how the mixing angle  $\theta_{13}$  depends on other parameters and whether  $CP$  violation is realized. In the upper left panel of Fig. 4, the data points indicate how the mixing angle  $\theta_{13}$  is determined in terms of the ratio  $y_1/y_2$ . We see that the measured value of  $\theta_{13}$  in  $3\sigma$ , including the Daya

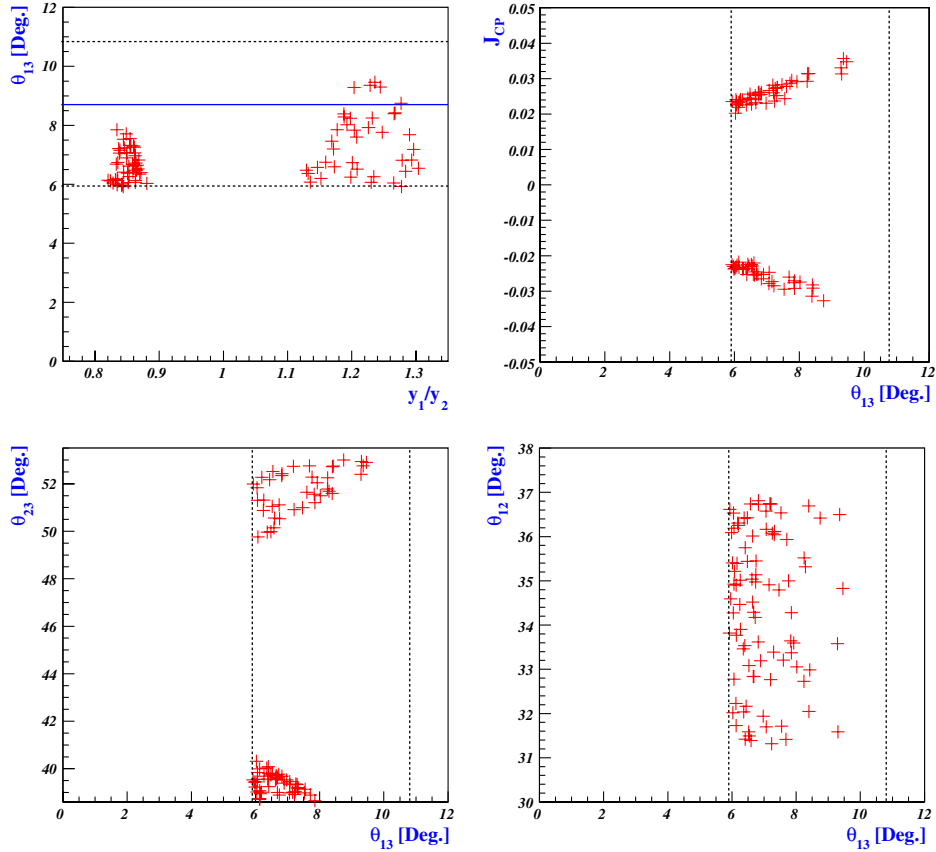


FIG. 4 (color online). Same as Fig. 2 for case (ii).

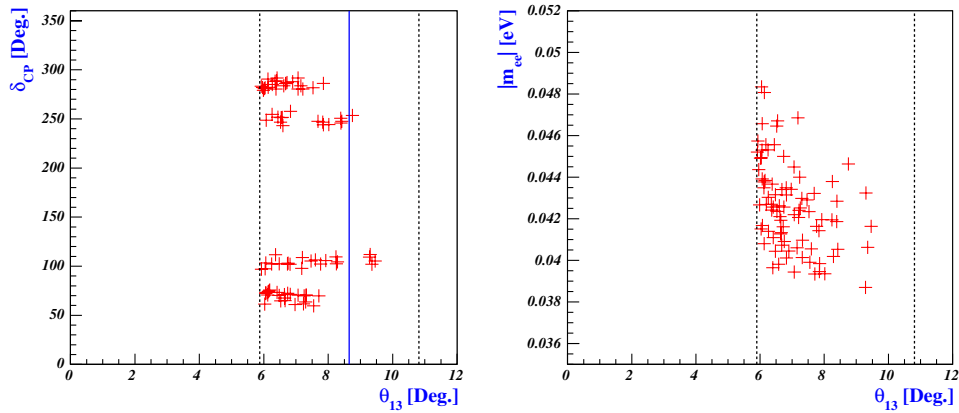


FIG. 5 (color online). Same as Fig. 3 for case (ii).

Bay experiment in Eq. (2), can be achieved for two separate regions,  $0.82 < y_1/y_2 < 0.88$  and  $1.12 \leq y_1/y_2 \leq 1.3$ . We plot  $J_{CP}$  versus  $\theta_{13}$  in the upper right panel of Fig. 4. For  $5.9^\circ \leq \theta_{13} \leq 9.5^\circ$ ,  $|J_{CP}| \approx 0.018 \sim 0.036$  and  $-0.02 \sim -0.034$ , which indicates  $CP$  violation in the leptonic sector.

In the lower panels of Fig. 4, the data points show how  $\theta_{13}$  is determined in the allowed regions of  $\theta_{12}$  and  $\theta_{23}$  given by Eq. (3). We see that the narrowed regions of the atmospheric mixing angle  $\theta_{23}$ ,  $38.6^\circ \leq \theta_{23} \leq 40.5^\circ$  and  $49.5^\circ \leq \theta_{23} \leq 53.1^\circ$ , are preferred, which indicates that the parameter set disfavors maximal mixing for the atmospheric mixing angles. From the lower right panel of Fig. 4, we see that determination of  $\theta_{13}$  does not strongly depend on  $\theta_{12}$  for the allowed region. We see from the figures that contrary to case (i),  $\theta_{13}$  for the inverted hierarchy prefers rather lower values of less than  $9.5^\circ$ . The left panel of Fig. 5 shows that  $\delta_{CP}$  is predicted to be around 70, 100, 160, 250, and  $290^\circ$ . In the right panel of Fig. 5, the value of  $|m_{ee}|$  is predicted as a function of  $\theta_{13}$  and we see that  $|m_{ee}|[\text{eV}]$  lies between 0.038 and 0.049 in the allowed region of  $\theta_{13}$ .

## V. CONCLUSION

Motivated by recent observations of nonzero  $\theta_{13}$  from the Daya Bay and RENO experiments, we have proposed in this paper a neutrino model with  $A_4$  symmetry and shown how deviations from the TBM mixing indicated by the current neutrino data, including the Daya Bay result, can be accounted for. In addition to the leptons and the Higgs scalar of the SM, our model contains three right-handed heavy Majorana neutrinos and several scalar fields which are electroweak singlets required to construct desirable forms of the leptonic mass matrices. To have a good dark matter candidate, we imposed auxiliary  $Z_2$  symmetry,

and thus light neutrino masses at tree level are absent in our model. However, the light neutrino masses can be generated through a loop diagram, and we have shown how the light neutrino mass matrix can be diagonalized by the PMNS mixing matrix whose entries are determined by the current neutrino data, including the Daya Bay result. In our model, the origin of the deviations from TBM mixing is nondegenerate neutrino Yukawa coupling constants among three generations. Also, unremovable  $CP$  phases in the neutrino Yukawa matrix are the origin of the low energy  $CP$  violation measurable from neutrino oscillation and high energy  $CP$  violation. We have discussed some implications on leptonic  $CP$  violation.

## ACKNOWLEDGMENTS

The work of S. K. Kang was supported in part by the National Research Foundation of Korea (NRF) grant funded by the Korea government of the Ministry of Education, Science and Technology (MEST) (No. 2011-0003287).

## APPENDIX: THE HIGGS MASS

Our model contains four Higgs doublets and three Higgs singlets. Here, we present the masses of physical scalar bosons, where the standard Higgs  $h'$  is mixed with  $\chi'_{0i}$ , not with  $h'_i, A'_i$ . For simplicity, we assume that  $CP$  is conserved in the scalar potential, and then the coupling  $\lambda_3^{\eta\Phi}$  is real and the term  $\xi_2^{\eta\chi}(\eta^\dagger\eta)_{3_a}\chi$  is neglected in the Higgs potential given in Eq. (10). The neutral Higgs boson mass matrix in the basis of  $(h', \chi'_{01}, \chi'_{02}, \chi'_{03}, h'_1, h'_2, h'_3, A'_1, A'_2, A'_3)$  is block diagonalized due to  $Z_2$  symmetry and  $CP$  conservation, which is given by

$$M_{\text{neutral}}^2 = \begin{pmatrix} m_{h'}^2 & m_{h'\chi'_1}^2 & 0 & 0 & 0 & 0 & 0 & 0 & 0 & 0 \\ m_{h'\chi'_1}^2 & m_{\chi'_1}^2 & 0 & 0 & 0 & 0 & 0 & 0 & 0 & 0 \\ 0 & 0 & m_{\chi'_2}^2 & m_{\chi'_2\chi'_3}^2 & 0 & 0 & 0 & 0 & 0 & 0 \\ 0 & 0 & m_{\chi'_2\chi'_3}^2 & m_{\chi'_3}^2 & 0 & 0 & 0 & 0 & 0 & 0 \\ 0 & 0 & 0 & 0 & m_{h'_1}^2 & 0 & 0 & 0 & 0 & 0 \\ 0 & 0 & 0 & 0 & 0 & m_{h'_2}^2 & m_{h'_2h'_3}^2 & 0 & 0 & 0 \\ 0 & 0 & 0 & 0 & 0 & m_{h'_3h'_2}^2 & m_{h'_3}^2 & 0 & 0 & 0 \\ 0 & 0 & 0 & 0 & 0 & 0 & 0 & m_{A'_1}^2 & 0 & 0 \\ 0 & 0 & 0 & 0 & 0 & 0 & 0 & 0 & m_{A'_2}^2 & m_{A'_2A'_3}^2 \\ 0 & 0 & 0 & 0 & 0 & 0 & 0 & 0 & m_{A'_3A'_2}^2 & m_{A'_3}^2 \end{pmatrix}, \quad (\text{A1})$$

where the primed particles are not mass eigenstates, and mass parameters are given as

$$\begin{aligned}
m_{h'}^2 &= 4\lambda^\Phi v_\Phi^2, & m_{h'\chi'_1}^2 &= 2v_\Phi v_\chi \lambda^{\Phi\chi}, & m_{\chi'_1}^2 &= 4v_\chi^2(\lambda_1^\chi + \lambda_2^\chi), & m_{\chi'_{2(3)}}^2 &= v_\chi^2(3\lambda_2^\chi + 4\lambda_3^\chi), & m_{\chi'_{2\chi'_3}}^2 &= 3v_\chi \xi_1^\chi \\
m_{h'_1}^2 &= v_\Phi^2(\lambda_1^{\eta\Phi} + \lambda_2^{\eta\Phi} + 2\lambda_3^{\eta\Phi}) + \mu_\eta^2 + v_\chi^2(\lambda_1^{\eta\chi} + 2\text{Re}[\lambda_2^{\eta\chi}]), \\
m_{A'_1}^2 &= v_\Phi^2(\lambda_1^{\eta\Phi} + \lambda_2^{\eta\Phi} - 2\lambda_3^{\eta\Phi}) + \mu_\eta^2 + v_\chi^2(\lambda_1^{\eta\chi} + 2\text{Re}[\lambda_2^{\eta\chi}]), \\
m_{h'_2}^2 &= v_\Phi^2(\lambda_1^{\eta\Phi} + \lambda_2^{\eta\Phi} + 2\lambda_3^{\eta\Phi}) + \mu_\eta^2 + v_\chi^2(\lambda_1^{\eta\chi} - \text{Re}[\lambda_2^{\eta\chi}] - \sqrt{3}\text{Im}[\lambda_2^{\eta\chi}]), \\
m_{h'_3}^2 &= v_\Phi^2(\lambda_1^{\eta\Phi} + \lambda_2^{\eta\Phi} + 2\lambda_3^{\eta\Phi}) + \mu_\eta^2 + v_\chi^2(\lambda_1^{\eta\chi} - \text{Re}[\lambda_2^{\eta\chi}] + \sqrt{3}\text{Im}[\lambda_2^{\eta\chi}]), \\
m_{A'_2}^2 &= v_\Phi^2(\lambda_1^{\eta\Phi} + \lambda_2^{\eta\Phi} - 2\lambda_3^{\eta\Phi}) + \mu_\eta^2 + v_\chi^2(\lambda_1^{\eta\chi} - \text{Re}[\lambda_2^{\eta\chi}] - \sqrt{3}\text{Im}[\lambda_2^{\eta\chi}]), \\
m_{A'_3}^2 &= v_\Phi^2(\lambda_1^{\eta\Phi} + \lambda_2^{\eta\Phi} - 2\lambda_3^{\eta\Phi}) + \mu_\eta^2 + v_\chi^2(\lambda_1^{\eta\chi} - \text{Re}[\lambda_2^{\eta\chi}] + \sqrt{3}\text{Im}[\lambda_2^{\eta\chi}]), \\
m_{h'_2 h'_3}^2 &= m_{A'_2 A'_3}^2 = v_\chi \xi_1^{\eta\chi}.
\end{aligned} \tag{A2}$$

Since the matrix in Eq. (A1) is block diagonalized, it is easy to obtain the mass spectrum given as follows:

$$\begin{aligned}
m_h^2 &= \frac{1}{2} \left\{ m_{h'}^2 + m_{\chi'_1}^2 - \sqrt{(m_{h'}^2 - m_{\chi'_1}^2)^2 + 4(m_{h'\chi'_1}^2)^2} \right\}, \\
m_{\chi_1}^2 &= \frac{1}{2} \left\{ m_{h'}^2 + m_{\chi'_1}^2 + \sqrt{(m_{h'}^2 - m_{\chi'_1}^2)^2 + 4(m_{h'\chi'_1}^2)^2} \right\}, \\
m_{\chi_2}^2 &= m_{\chi'_2}^2 - m_{\chi'_2 \chi'_3}^2, & m_{\chi_3}^2 &= m_{\chi'_2}^2 + m_{\chi'_2 \chi'_3}^2, & m_{h_1}^2 &= m_{h'_1}^2, & m_{A_1}^2 &= m_{A'_1}^2, \\
m_{h_2}^2 &= v_\Phi^2(\lambda_{12}^{\eta\Phi} + 2\lambda_3^{\eta\Phi}) + \mu_\eta^2 + v_\chi^2(\lambda_1^{\eta\chi} - \text{Re}[\lambda_2^{\eta\chi}]) - v_\chi \sqrt{3(v_\chi \text{Re}[\lambda_2^{\eta\Phi}])^2 + (\xi_1^{\eta\chi})^2}, \\
m_{A_2}^2 &= v_\Phi^2(\lambda_{12}^{\eta\Phi} - 2\lambda_3^{\eta\Phi}) + \mu_\eta^2 + v_\chi^2(\lambda_1^{\eta\chi} - \text{Re}[\lambda_2^{\eta\chi}]) - v_\chi \sqrt{3(v_\chi \text{Re}[\lambda_2^{\eta\Phi}])^2 + (\xi_1^{\eta\chi})^2}, \\
m_{h_3}^2 &= v_\Phi^2(\lambda_{12}^{\eta\Phi} + 2\lambda_3^{\eta\Phi}) + \mu_\eta^2 + v_\chi^2(\lambda_1^{\eta\chi} - \text{Re}[\lambda_2^{\eta\chi}]) + v_\chi \sqrt{3(v_\chi \text{Re}[\lambda_2^{\eta\Phi}])^2 + (\xi_1^{\eta\chi})^2}, \\
m_{A_3}^2 &= v_\Phi^2(\lambda_{12}^{\eta\Phi} - 2\lambda_3^{\eta\Phi}) + \mu_\eta^2 + v_\chi^2(\lambda_1^{\eta\chi} - \text{Re}[\lambda_2^{\eta\chi}]) + v_\chi \sqrt{3(v_\chi \text{Re}[\lambda_2^{\eta\Phi}])^2 + (\xi_1^{\eta\chi})^2},
\end{aligned} \tag{A3}$$

where  $\lambda_{12}^{\eta\Phi} \equiv \lambda_1^{\eta\Phi} + \lambda_2^{\eta\Phi}$ . Note here that the unprimed particles denote mass eigenstates. And the charged Higgs boson mass matrix in the basis of  $(\eta_1^\pm, \eta_2^\pm, \eta_3^\pm)$  is given as

$$m_{\text{charged}}^2 = \begin{pmatrix} m_{\eta_1^\pm}^2 & 0 & 0 \\ 0 & m_{\eta_2^\pm}^2 & 0 \\ 0 & 0 & m_{\eta_3^\pm}^2 \end{pmatrix}, \tag{A4}$$

where

$$\begin{aligned}
m_{\eta_1^\pm}^2 &= \mu_\eta^2 + v_\Phi^2 \lambda_1^{\eta\Phi} + v_\chi^2(\lambda_1^{\eta\chi} + 2\text{Re}[\lambda_2^{\eta\chi}]), \\
m_{\eta_2^\pm}^2 &= \mu_\eta^2 + v_\Phi^2 \lambda_1^{\eta\Phi} + v_\chi^2(\lambda_1^{\eta\chi} - \text{Re}[\lambda_2^{\eta\chi}] - \sqrt{3}\text{Im}[\lambda_2^{\eta\chi}]), \\
m_{\eta_3^\pm}^2 &= \mu_\eta^2 + v_\Phi^2 \lambda_1^{\eta\Phi} + v_\chi^2(\lambda_1^{\eta\chi} - \text{Re}[\lambda_2^{\eta\chi}] + \sqrt{3}\text{Im}[\lambda_2^{\eta\chi}]).
\end{aligned} \tag{A5}$$

Using  $m_{h'_i}^2, m_{A'_i}^2$  in Eqs. (A2) and (A4), the expressions for  $\bar{m}_{\eta_i}^2$  that appear in Eq. (24) are

$$\begin{aligned}
\bar{m}_{\eta_1}^2 &= \mu_\eta^2 + v_\Phi^2 \lambda_{12}^{\eta\Phi} + v_\chi^2(\lambda_1^{\eta\chi} + 2\text{Re}[\lambda_2^{\eta\chi}]) = m_{\eta_1^\pm}^2 + v_\Phi^2 \lambda_2^{\eta\Phi}, \\
\bar{m}_{\eta_2}^2 &= v_\Phi^2 \lambda_{12}^{\eta\Phi} + \mu_\eta^2 + v_\chi^2(\lambda_1^{\eta\chi} - \text{Re}[\lambda_2^{\eta\chi}] - \sqrt{3}\text{Im}[\lambda_2^{\eta\chi}]) = m_{\eta_2^\pm}^2 + v_\Phi^2 \lambda_2^{\eta\Phi}, \\
\bar{m}_{\eta_3}^2 &= v_\Phi^2 \lambda_{12}^{\eta\Phi} + \mu_\eta^2 + v_\chi^2(\lambda_1^{\eta\chi} - \text{Re}[\lambda_2^{\eta\chi}] + \sqrt{3}\text{Im}[\lambda_2^{\eta\chi}]) = m_{\eta_3^\pm}^2 + v_\Phi^2 \lambda_2^{\eta\Phi}.
\end{aligned} \tag{A6}$$

- [1] F.P. An *et al.* (DAYA-BAY Collaboration), *Phys. Rev. Lett.* **108**, 171803 (2012).
- [2] S.-B. Kim *et al.* (RENO Collaboration), *Phys. Rev. Lett.* **108**, 191802 (2012).
- [3] K. Abe *et al.* (T2K Collaboration), *Phys. Rev. Lett.* **107**, 041801 (2011); P. Adamson *et al.* (MINOS Collaboration), *Phys. Rev. Lett.* **107**, 181802 (2011); H. De Kerret *et al.* (Double Chooz Collaboration), *Sixth International Workshop on Low Energy Neutrino Physics* (Seoul National University, Seoul, Korea, 2011).
- [4] P. A. N. Machado, H. Minakata, H. Nunokawa, and R. Z. Funchal, *J. High Energy Phys.* **05** (2012) 023.
- [5] T. Schwetz, M. Tortola, and J. W. F. Valle, *New J. Phys.* **13**, 109401 (2011); see also M. C. Gonzalez-Garcia, M. Maltoni, and J. Salvado, *J. High Energy Phys.* **04** (2010) 056; G. L. Fogli, E. Lisi, A. Marrone, A. Palazzo, and A. M. Rotunno, *Phys. Rev. D* **84**, 053007 (2011).
- [6] P. F. Harrison, D. H. Perkins, and W. G. Scott, *Phys. Lett. B* **530**, 167 (2002); Z. Z. Xing, *Phys. Lett. B* **533**, 85 (2002); P. F. Harrison and W. G. Scott, *Phys. Lett. B* **535**, 163 (2002); X. G. He and A. Zee, *Phys. Lett. B* **560**, 87 (2003).
- [7] S. K. Kang, Z.-z. Xing, and S. Zhou, *Phys. Rev. D* **73**, 013001 (2006); Z.-z. Xing, H. Zhang, and S. Zhou, *Phys. Lett. B* **641**, 189 (2006); N. N. Singh, M. Rajkhowa, and A. Borah *Pramana* **69**, 533 (2007); M. Honda and M. Tanimoto, *Prog. Theor. Phys.* **119**, 583 (2008); S. F. King, *Phys. Lett. B* **659**, 244 (2008); A. Hayakawa, H. Ishimori, Y. Shimizu, and M. Tanimoto, *Phys. Lett. B* **680**, 334 (2009); S. F. King, *Phys. Lett. B* **675**, 347 (2009); S. Boudjemaa and S. F. King, *Phys. Rev. D* **79**, 033001 (2009); S. Antusch, S. F. King, and M. Malinsky, *Phys. Lett. B* **671**, 263 (2009); A. Adulpravitchai, M. Lindner, and A. Merle, *Phys. Rev. D* **80**, 055031 (2009); Y. F. Li and Q. Y. Liu, *Mod. Phys. Lett. A* **25**, 63 (2010); Y. H. Ahn and C. S. Chen, *Phys. Rev. D* **81**, 105013 (2010); M. Hirsch, S. Morisi, E. Peinado, and J. W. F. Valle, *Phys. Rev. D* **82**, 116003 (2010); S. F. King, *J. High Energy Phys.* **01** (2011) 115; T. Araki, J. Mei, and Z.-z. Xing, *Phys. Lett. B* **695**, 165 (2011); H.-J. He and F.-R. Yin, *Phys. Rev. D* **84**, 033009 (2011); Y. H. Ahn, C. S. Kim, and S. Oh, *Phys. Rev. D* **86**, 013007 (2012); Z.-Z. Xing, *Chinese Phys. C* **36**, 101 (2012); N. Qin and B. Q. Ma, *Phys. Lett. B* **702**, 143 (2011); Y. j. Zheng and B. Q. Ma, *Eur. Phys. J. Plus* **127**, 7 (2012); E. Ma and D. Wegman, *Phys. Rev. Lett.* **107**, 061803 (2011); X.-G. He and A. Zee, *Phys. Rev. D* **84**, 053004 (2011); S. Zhou, *Phys. Lett. B* **704**, 291 (2011); T. Araki, *Phys. Rev. D* **84**, 037301 (2011); N. Haba and R. Takahashi, *Phys. Lett. B* **702**, 388 (2011); D. Meloni, *J. High Energy Phys.* **10** (2011) 010; W. Chao and Y.-J. Zheng, *arXiv:1107.0738*; H. Zhang and S. Zhou, *Phys. Lett. B* **704**, 296 (2011); X. Chu, M. Dhen, and T. Hambye, *J. High Energy Phys.* **11** (2011) 106; P. S. Bhupal Dev, R. N. Mohapatra, and M. Severson, *Phys. Rev. D* **84**, 053005 (2011); R. d. A. Toorop, F. Feruglio, and C. Hagedorn, *Phys. Lett. B* **703**, 447 (2011); S. Antusch and V. Maurer, *Phys. Rev. D* **84**, 117301 (2011); S. F. King and C. Luhn, *J. High Energy Phys.* **09** (2011) 042; Q.-H. Cao, S. Khalil, E. Ma, and H. Okada, *Phys. Rev. D* **84**, 071302 (2011); D. Marzocca, S. T. Petcov, A. Romanino, and M. Spinrath, *J. High Energy Phys.* **11** (2011) 009; S. F. Ge, D. A. Dicus, and W. W. Repko, *Phys. Rev. Lett.* **108**, 041801 (2012); F. Bazzocchi, *arXiv:1108.2497*; S. Antusch, S. F. King, C. Luhn, and M. Spinrath, *Nucl. Phys.* **B856**, 328 (2012); P. O. Ludl, S. Morisi, and E. Peinado, *Nucl. Phys.* **B857**, 411 (2012); A. Aranda, C. Bonilla, and A. D. Rojas, *Phys. Rev. D* **85**, 036004 (2012); D. Meloni, *J. High Energy Phys.* **02** (2012) 090; Y. H. Ahn, H. Y. Cheng, and S. Oh, *Phys. Rev. D* **83**, 076012 (2011); M. S. Boucenna, M. Hirsch, S. Morisi, E. Peinado, M. Taoso, and J. W. F. Valle, *J. High Energy Phys.* **05** (2011) 037; S. Morisi, K. M. Patel, and E. Peinado, *Phys. Rev. D* **84**, 053002 (2011); I. de Medeiros Varzielas, *J. High Energy Phys.* **01** (2012) 097; S. Dev, S. Gupta, R. R. Gautam, and L. Singh, *Phys. Lett. B* **706**, 168 (2011); A. Rashed, *Phys. Rev. D* **85**, 035019 (2012); R. d. A. Toorop, F. Feruglio, and C. Hagedorn, *Nucl. Phys.* **B858**, 437 (2012); Y. H. Ahn and H. Okada, *Phys. Rev. D* **85**, 073010 (2012); S. F. King and C. Luhn, *J. High Energy Phys.* **03** (2012) 036; S. Gupta, A. S. Joshipura, and K. M. Patel, *Phys. Rev. D* **85**, 031903 (2012); Y.-L. Wu, *Phys. Lett. B* **714**, 286 (2012); G.-J. Ding, *Nucl. Phys.* **B862**, 1 (2012); I. K. Cooper, S. F. King, and C. Luhn, *J. High Energy Phys.* **06** (2012) 130; Kim Siyeon, *Eur. Phys. J. C* **72**, 2081 (2012); Z.-z. Xing, *Chinese Phys. C* **36**, 281 (2012); G. C. Branco, R. Gonzalez Felipe, F. R. Joaquim, and H. Serodio, *arXiv:1203.2646*; H.-J. He and X.-J. Xu, *arXiv:1203.2908*; S. Luo and Z.-z. Xing, *arXiv:1203.3118*; D. Meloni, *J. High Energy Phys.* **05** (2012) 124.
- [8] E. Ma, *Mod. Phys. Lett. A* **21**, 1777 (2006).
- [9] E. Ma and G. Rajasekaran, *Phys. Rev. D* **64**, 113012 (2001); K. S. Babu, E. Ma, and J. W. F. Valle, *Phys. Lett. B* **552**, 207 (2003); M. Hirsch, J. C. Romao, S. Skadhauge, J. W. F. Valle, and A. Villanova del Moral, *arXiv:hep-ph/0312244*; M. Hirsch, J. C. Romao, S. Skadhauge, J. W. F. Valle, and A. Villanova del Moral, *Phys. Rev. D* **69**, 093006 (2004); E. Ma, *Phys. Rev. D* **70**, 031901 (2004); *arXiv:hep-ph/0409075*; *New J. Phys.* **6**, 104 (2004); G. Altarelli and F. Feruglio, *Nucl. Phys.* **B720**, 64 (2005).
- [10] K. Nakamura *et al.* (Particle Data Group), *J. Phys. G* **37**, 075021 (2010), and 2011 partial update for the 2012 edition.
- [11] S. Antusch, J. Kersten, M. Lindner, M. Ratz, and M. A. Schmidt, *J. High Energy Phys.* **03** (2005) 024.
- [12] C. Jarlskog, *Phys. Rev. Lett.* **55**, 1039 (1985); D. d. Wu, *Phys. Rev. D* **33**, 860 (1986).
- [13] G. C. Branco, R. Gonzalez Felipe, F. R. Joaquim, I. Masina, M. N. Rebelo, and C. A. Savoy, *Phys. Rev. D* **67**, 073025 (2003).